Journal of Alloys and Compounds 424 (2006) 350–355

Journal of ALLOYS AND COMPOUNDS

www.elsevier.com/locate/jallcom

Corrosion behavior of bulk metallic glass $Pr_{60}Fe_{30-x}TM_xAl_{10}$ in NaCl aqueous solution

Qingge Meng[a,*], Jianguo Li[a], Xiufang Bian[b]

[a] School of Materials Science and Engineering, Shanghai Jiao Tong University, Shanghai 200030, China
[b] Key Lab of Liquid Structure and Heredity of Materials, Ministry of Education, Shandong University, Jinan 250061, China

Received 18 October 2005; received in revised form 16 November 2005; accepted 21 December 2005

Abstract

In this paper, Mn, Ni, Cu and Ti were selected as the partial substitution elements for Fe to produce $Pr_{60}Fe_{30-x}TM_xAl_{10}$ (TM = Mn, Ni, Cu, Ti; $x = 0$, 5 at.%) quaternary bulk metallic glasses (BMGs) by copper mold casting. The microstructure of samples was characterized by X-ray diffraction (XRD) and the effects of substitution elements on glass forming ability (GFA), electrochemical corrosion behavior in 3.5 wt.% NaCl solution were investigated by differential scanning calorimetry (DSC), potentiodynamic polarization and electrochemical impedance spectroscopic (EIS) techniques. The thermal parameters (e.g. T_x/T_l, γ, G_s, etc.) deduced from DSC indicated that all the samples possessed an amorphous phase and had a high GFA, the GFA of the samples ranks from high to low in the order: $Pr_{60}Fe_{25}Mn_5Al_{10} > Pr_{60}Fe_{30}Al_{10} > Pr_{60}Fe_{25}Ni_5Al_{10} > Pr_{60}Fe_{25}Ti_5Al_{10} > Pr_{60}Fe_{25}Cu_5Al_{10}$ and the potentiodynamic polarization data analysis shows that the corrosion resistance ability ranks: $Pr_{60}Fe_{25}Mn_5Al_{10} < Pr_{60}Fe_{30}Al_{10} < Pr_{60}Fe_{25}Ni_5Al_{10} < Pr_{60}Fe_{25}Cu_5Al_{10} < Pr_{60}Fe_{25}Ti_5Al_{10}$, which agrees well with that of the EIS data. In the case of the Pr-based BMGs, the GFA has not a correlation with the corrosion resistance, however the chemical composition is the dominating factor controlling the relative corrosion resistance.

Keywords: Pr-based amorphous alloys; Corrosion behavior; Glass forming ability; Potentiodynamic polarization; Electrochemical impedance spectroscopy

---

1. Introduction

Since the first "bulk metallic glass" (BMG) Pd–Cu–Si was prepared by Chen in 1974 [1], it trigged a revolution in BMG research and development. The work of Inoue et al. opened the door to the design of new families of BMGs and the three empirical rules advocated by him were one of the most effective ways to find new BMG systems [2]. At the same time, a variety of amorphization techniques based on completely different mechanism from rapid quenching, such as mechanical alloying, diffusion induced amorphization in multilayers, ion beam mixing, hydrogen absorption and inverse melting had been developed [3]. On account of the unique and unconventional characteristics, BMG materials are adopted for applications in various fields and conditions. The ferrous-group-based and rare earth-based alloy systems, e.g. Pr–Fe–Al and Nd–Fe–Al, have received much attention on the rather good soft and hard magnetic properties [4,5].

While the magnetic properties, crystallization kinetics and structural changes of Nd–TM–Al alloys have been studied extensively, little information is available on the Pr–TM–Al systems, especially the information of electrochemical properties. The partial substitution of other transition metals for $Pr_{60}Fe_{30-x}TM_xAl_{10}$ (TM = Mn, Ni, Cu, Ti; $x = 0$, 5 at.%) appears specially interesting regarding the GFA and corrosion resistance. As GFA is very crucial for understanding the origins of glass formation and also important for designing and developing new bulk metallic glasses, a great deal of effort has therefore been devoted to searching for a simple and reliable gauge for qualifying GFA [5–7]. Furthermore, the superior corrosion resistance of the amorphous alloys has also caught much attention on their special structures. By Tafel experiments, Alvarez et al. [8] had explored the corrosion behavior of Ni–B–Sn melt-spun amorphous ribbons in 1 M NaCl solution with different pH values and concluded that this amorphous alloys exhibit a better corrosion resistance than their crystalline counterparts; however the corrosion behavior of amorphous alloys is primarily determined by the character of the alloying elements; Liu and co-workers [9] also used the potentiodynamic anodic polarization method

---

[*] Corresponding author. Tel.: +86 21 62932569; fax: +86 21 62933074.
E-mail address: mggsjtu@sjtu.edu.cn (Q. Meng).

0925-8388/$ – see front matter © 2006 Elsevier B.V. All rights reserved.
doi:10.1016/j.jallcom.2005.12.081

to study the corrosion behavior of the $Zr_{52.5}Cu_{17.9}Ni_{14.6}Al_{10}Ti_5$ BMGs in different solutions and concluded that there is a correlation between the corrosion resistance and the solution types; Qin et al. [10] used XRD, EIS and X-ray photoelectron spectroscopy (XPS) to monitor the corrosion behavior of BMG $Zr_{55}Al_{10}Cu_{30}Ni_{5-x}Pd_x$ ($x = 0$, 5 at.%), the results showed that different corrosion behavior originated from different GFA; Hu et al. made a comparative study on the corrosion behavior of BMG Cu–Zr–Ti–Sn and its crystallized form in 3.5 wt.% NaCl solution by potentiodynamic polarization and EIS techniques. However, the combined study techniques of EIS and Tafel experiments in previous works have not been discussed quantitatively on corrosion mechanism, even little information on corrosion behavior of Pr-based BMGs is reported. Further, for more BMG samples with different GFA, is there still a correlation between the GFA and corrosion behavior? Therefore, in this work, the key BMG temperatures (T_x, T_m, T_l, etc.) of $Pr_{60}Fe_{30-x}TM_xAl_{10}$, which are often used to characterize vitrification and properties of a glass, are determined, a EIS equivalent circuit model is established and the corrosion mechanism is discussed from a comparative study of Tafel and EIS experiments.

2. Experimental

Alloys with the nominal atomic percent compositions of $Pr_{60}Fe_{30-x}TM_xAl_{10}$ (TM = Mn, Ni, Cu, Ti; $x = 0$, 5) were prepared by arc melting Fe, Mn, Cu, Ni and Ti with the purity of no less than 99.9 wt.% and Pr with the purity of no less than 99.7 wt.% in titanium-gettered argon atmosphere. Cylindrical specimens of 3 mm in diameter and 80 mm in length were prepared from the pre-alloys ingots by suction casting into a copper mold; thermal analysis was performed with a Netzsch DSC 404C calorimeter using pure indium (99.999 wt.%) and zinc (99.999 wt.%) standards and a sample of 20 ± 0.5 mg, all the DSC measurements were conducted in a flowing (60 cm^3/min) argon gas; the microstructure of the cast cylinders was examined by XRD in a D/Max-rB diffractometer using Cu Kα radiation, the scattering angle (2θ) range is 5–80°.

The cylindrical specimens were grinded into 0.2 cm × 0.5 cm areas at one end and a copper wire lead was attached with the silver paint to the other end. Except for the exposed areas for testing, all the specimen surfaces were covered with an epoxy resin, next, the testing areas were mechanically polished with successive SiC papers of 240, 400 and 600 grain size, then degreased with ethyl acetate and washed with ethyl alcohol and distilled water before each experiment. Electrochemical measurements were obtained using a typical three-electrode system: a stationary specimen, a pair of counter electrodes (consists of a Pt sheet) and a saturated calomel reference electrode (SCE). A CHI 660B electrochemical workstation was used for the polarization curves and EIS measurement at room temperature after 20 min exposure to the test solution starting at the open-circuit potential. The test solution, 3.5 wt.% NaCl aqueous solution, was prepared with analytical grade NaCl reagent (≥99.5 wt.%) and deionized water. A scan rate of 0.8 mV/s was used for the potentiodynamic polarization test. The EIS method was used in the frequency range from 10^5 to 0.1 Hz and involved the imposition of a 5 mV amplitude sinewave. From potentiodynamic polarization curves and EIS results, the parameters related to corrosion were obtained to investigate the electrochemical behaviors of these BMGs.

3. Results and discussion

3.1. Formation of $Pr_{60}Fe_{30-x}TM_xAl_{10}$ (TM = Mn, Ni, Cu, Ti; $x = 0$, 5) BMGs

Fig. 1 shows the XRD patterns of the as-cast $Pr_{60}Fe_{30-x}TM_xAl_{10}$ BMGs in cylindrical shapes, revealing the characteristic broad diffraction peaks around 2θ from 25 to 40° and no clearly visible diffraction peaks corresponding to crystalline phases, all of the specimens exhibit a fully amorphous structure, furthermore the profiles of the XRD patterns are similar, indicating that the $Pr_{60}Fe_{30-x}TM_xAl_{10}$ BMGs have a similar amorphous structure.

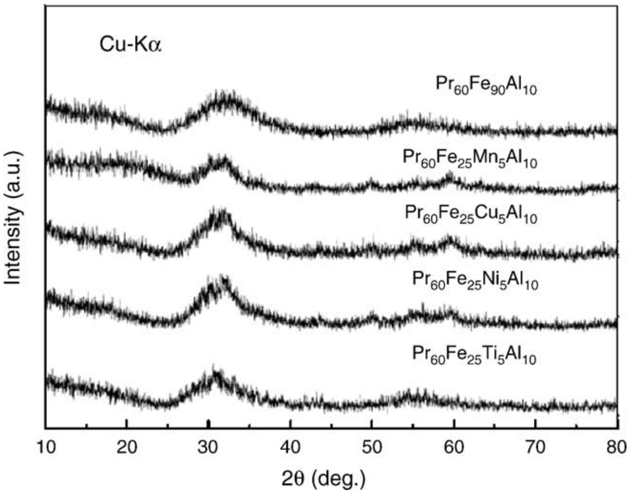

Fig. 1. XRD patterns of the as-cast $Pr_{60}Fe_{30-x}TM_xAl_{10}$ (TM = Mn, Ni, Cu, Ti; $x = 0$, 5) BMG rods with the diameter of 3 mm.

Fig. 2 shows typical examples of DSC results for the as-cast $Pr_{60}Fe_{30-x}TM_xAl_{10}$ BMGs in cylindrical shapes, examined at a heating rate of 10 K/min. It can be seen from Fig. 2 that all the DSC curves consist of only exothermic peaks due to crystallization and endothermic peaks due to melting, Neither appreciable endothermic reaction due to glass transition nor the subsequent supercooled liquid region is found in the temperature range before crystallization. This absence of a glass transition phenomenon is similar to what occurs for Nd–Fe–Al BMGs [5]. Fig. 2 shows that T_m and T_l vary strongly as the alloy compositions change by replacing the Fe with TM. The onset temperature of crystallization T_x, onset melting temperature T_m, offset melting temperature T_l (i.e. the liquidus temperature), enthalpy of

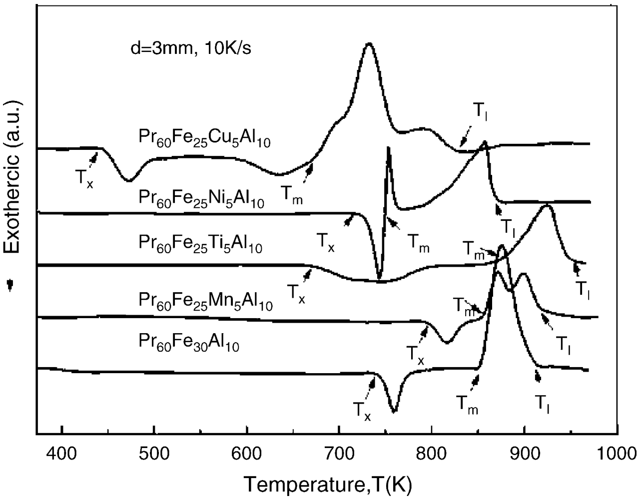

Fig. 2. DSC curves of the as-cast $Pr_{60}Fe_{30-x}TM_xAl_{10}$ (TM = Mn, Ni, Cu, Ti; $x = 0$, 5) BMGs in the diameter of 3 mm.